bioRxiv preprint doi: https://doi.org/10.1101/2021.11.25.470003; this version posted November 25, 2021. The copyright holder for this preprint (which was not certified by peer review) is the author/funder, who has granted bioRxiv a license to display the preprint in perpetuity. It is made available under aCC-BY-NC-ND 4.0 International license.

SRSF3 is a key regulator of epicardial formation

Irina-Elena Lupu,[1] Andia N. Redpath [1,2] and Nicola Smart [1,2]

[1]Department of Physiology, Anatomy & Genetics, University of Oxford, Oxford OX1 3PT, UK.

[2]These authors contributed equally to this work.

Corresponding author: nicola.smart@dpag.ox.ac.uk

bioRxiv preprint doi: https://doi.org/10.1101/2021.11.25.470003; this version posted November 25, 2021. The copyright holder for this preprint (which was not certified by peer review) is the author/funder, who has granted bioRxiv a license to display the preprint in perpetuity. It is made available under aCC-BY-NC-ND 4.0 International license.

Abstract

The epicardium is a fundamental regulator of cardiac development, functioning to secrete essential growth factors and to produce epicardium-derived cells (EPDCs) that contribute most coronary vascular smooth muscle cells and cardiac fibroblasts. The molecular mechanisms that control epicardial formation and proliferation have not been fully elucidated. In this study, we found that the RNA-binding protein SRSF3 is highly expressed in the proepicardium and later in the epicardial layer during heart development. Deletion of *Srsf3* from the murine proepicardium using the *Tg(Gata5-Cre)* or embryonic day (E) 8.5 induction of *Wt1*^{CreERT2} led to proliferative arrest and impaired epithelial-to-mesenchymal transition (EMT), which prevented proper formation and function of the epicardial layer. Induction of *Srsf3* deletion with the *Wt1*^{CreERT2} after the proepicardial stage resulted in impaired EPDC formation and epicardial proliferation at E13.5. Single-cell RNA-sequencing showed SRSF3-depleted epicardial cells were removed by E15.5 and the remaining non-recombined cells became hyperproliferative and compensated for the loss via up-regulation of *Srsf3*. This research identifies SRSF3 as a master regulator of cellular proliferation in epicardial cells.

bioRxiv preprint doi: https://doi.org/10.1101/2021.11.25.470003; this version posted November 25, 2021. The copyright holder for this preprint (which was not certified by peer review) is the author/funder, who has granted bioRxiv a license to display the preprint in perpetuity. It is made available under aCC-BY-NC-ND 4.0 International license.

Introduction

Understanding cardiac morphogenesis is essential for designing improved therapies to treat heart disease. The outer layer of the heart, the epicardium, is a major player in cardiovascular regeneration, shown to promote cardiomyocyte proliferation and vessel growth in developing embryos and in species that regenerate their hearts, through providing growth factors and perivascular support (Lepilina et al. 2006; Kikuchi et al. 2011; Smart and Riley 2012; Wang et al. 2015; Cao et al. 2016; Dubé et al. 2017; Cao and Cao 2018; Redpath and Smart 2021). For non-regenerative species, maximising the therapeutic potential of the epicardium depends upon augmenting the restricted reactivation and proliferation that occur endogenously (Redpath and Smart 2021).

The epicardial layer originates from the proepicardial organ (PEO), a transient embryonic structure located at the venous pole of the developing heart (Schulte et al. 2007). After epicardial formation is complete, around embryonic day (E) 11.5 in mouse, some epicardial cells undergo epithelial-to-mesenchymal (EMT), leading to the formation of epicardium-derived cells (EPDCs) that contribute most vascular smooth muscle cells (vSMCs) and cardiac fibroblasts (CFs) to the developing heart (Mellgren et al. 2008; Smith et al. 2011; Rudat et al. 2013; Liu et al. 2016; Singh et al. 2016).

A key process in epicardial formation and function is cellular proliferation. PEO cluster emergence in zebrafish was shown to be dependent on tension generated through regionalised proliferation of mesodermal progenitors (Andrés-Delgado et al. 2019). Epicardial EMT (epiEMT) also requires cell division, with orientation of the mitotic spindle dictating which cells remain on the surface, versus which cells invade the myocardium (Wu et al. 2010). Studies where epicardial proliferation rate was increased by Cyclin D1 overexpression (Wu et al. 2010) or deletion of neurofibromin1 (NF1), a negative regulator of Ras, (Baek and Tallquist 2012) resulted in increased formation of EPDCs.

bioRxiv preprint doi: https://doi.org/10.1101/2021.11.25.470003; this version posted November 25, 2021. The copyright holder for this preprint (which was not certified by peer review) is the author/funder, who has granted bioRxiv a license to display the preprint in perpetuity. It is made available under aCC-BY-NC-ND 4.0 International license.

The RNA-binding protein Serine/arginine-rich splicing factor 3 (SRSF3) is the smallest member of the serine/arginine rich (SR) family of proteins, master regulators of RNA metabolism in the cell, involved in multiple aspects of RNA processing, such as mRNA transcription, splicing, export, stability and translation (Zahler et al. 1992; Shen et al. 2004; Shepard and Hertel 2009; Änkö et al. 2012; Kim et al. 2014; Müller-McNicoll et al. 2016; Park and Jeong 2016; Mure et al. 2018; Ratnadiwakara et al. 2018). SRSF3 is also labelled as an oncogene due to its role in promoting cellular proliferation and migration in various cancers (Corbo et al. 2013; Kano et al. 2013; Kurokawa et al. 2013; Tang et al. 2013; Sen et al. 2015; Park and Jeong 2016; Kim et al. 2017; Ke et al. 2018). Recently, SRSF3 was shown to be required for cardiomyocyte proliferation during development, with conditional deletion of SRSF3 in NKX2.5 or αMHC expressing cells resulting in embryonic lethality mid-gestation (Ortiz-Sánchez et al. 2019). The role of SRSF3 in the formation of the epicardium has not been previously investigated, but SRSF3 has been implicated in multiple developmental transitions (Jumaa et al. 1999; Änkö et al. 2010; Sen et al. 2013; Do et al. 2018).

Here, we show that SRSF3 is expressed ubiquitously in the heart during embryonic development, with the highest expression levels in the PEO and in the epicardium until E11.5. To address the role of SRSF3 in the epicardium, we generated two SRSF3 conditional-knockout mice. Deletion of SRSF3 using the Tg(Gata5-Cre) resulted in embryonic lethality at E12.5 and impaired epicardial layer formation, due to decreased proliferation of epicardial progenitor cells. Epicardial-specific deletion later in development, using the inducible Wt1CreERT2, resulted in a less severe phenotype characterised by impaired coronary vascular formation and reduced cardiac compaction due to defective epicardial proliferation and EMT. These data reveal an essential role for SRSF3 in the proliferation of (pro)epicardial cells and in the epicardial processes that underpin cardiac morphogenesis.

Results

Characterisation of SRSF3 expression during development

bioRxiv preprint doi: https://doi.org/10.1101/2021.11.25.470003; this version posted November 25, 2021. The copyright holder for this preprint (which was not certified by peer review) is the author/funder, who has granted bioRxiv a license to display the preprint in perpetuity. It is made available under aCC-BY-NC-ND 4.0 International license.

The expression pattern of SRSF3 at key stages of epicardial activity was investigated by immunohistochemistry (IHC) of mouse embryo and heart cryosections: at E9.5, when epicardial progenitors first arise within the proepicardial organ (PEO), at E11.5, when the epicardium is most proliferative and has formed a layer (Wu et al. 2010; Lupu et al. 2020b); and at E15.5 when the epicardium downregulates key epicardial genes (Lupu et al. 2020b) and progresses toward quiescence (Wu et al. 2010; Liu et al. 2016). Highest levels of SRSF3 were found in the PEO and in the early epicardium (E11.5), after which SRSF3 expression started to decrease (Fig.1A, B, Supplemental Fig. S1A) until postnatal stages, where SRSF3 levels were low (Supplemental Fig. S1B). Notably, reduction in SRSF3 expression levels coincided with the downregulation of Wilms' Tumor 1 (WT1) in the epicardium (Fig. 1A), a transcriptional regulator that marks the active epicardial state (Redpath and Smart 2021). Strong SRSF3 expression was maintained in E11.5 epicardial explant cultures (Fig. 1C), where outgrowth is governed by epicardial cell proliferation.

SRSF3 is required for epicardial formation and cardiomyocyte survival

To investigate the role of SRSF3 in the PEO, Tg(Gata5-Cre);Rosa26^{TdTomato} mice (Merki et al. 2005; Madisen et al. 2010) were crossed with Srsf3$^{fl/fl}$ mice (Ortiz-Sánchez et al. 2019) in order to deplete SRSF3 in epicardial progenitor cells, and concomitantly label them to track their migration (defined as *Srsf3* cKO; Fig.1D). Tg(Gata5-Cre) uses a chick enhancer of *Gata5* that becomes active at E9.25 and drives Cre recombinase expression in the PEO (Merki et al. 2005), septum transversum and a subset of cardiomyocytes (Vieira et al. 2017). *Srsf3* cKO displayed embryonic lethality from E12.5, with no live embryos recovered beyond this stage (Supplemental Table S1). E12.5 *Srsf3* cKO embryos presented gross morphological abnormalities of the heart, such as hypoplastic ventricles and dilated atria (Fig. 1E). Since the ventricles were smaller, cell death and proliferation were investigated by IHC. There was increased cell death and decreased proliferation in *Srsf3* cKO hearts, as indicated by cleaved-caspase 3 (CC3) and phospho-histone H3 (PHH3), respectively (Supplemental Fig. S1C-F). All the cells expressing CC3 were positive for sarcomeric-α-actinin (s-α-actinin), indicating that

bioRxiv preprint doi: https://doi.org/10.1101/2021.11.25.470003; this version posted November 25, 2021. The copyright holder for this preprint (which was not certified by peer review) is the author/funder, who has granted bioRxiv a license to display the preprint in perpetuity. It is made available under aCC-BY-NC-ND 4.0 International license.

SRSF3 is only required for cardiomyocyte survival (Supplemental Fig. S2C). There were fewer PHH3 positive tdTomato cells which consisted of both cardiomyocytes and epicardial cells (Supplemental Fig. S2E, F), indicating that SRSF3 is required for the proliferation of both cell types. The requirement for SRSF3 to enable cardiomyocyte proliferation in the developing embryo has been reported (Ortiz-Sánchez et al. 2019), however, the involvement of SRSF3 in epicardial proliferation has not been addressed.

To investigate the impact of SRSF3 depletion on epicardial formation, we immunostained E12.5 heart cryosections for WT1 (Fig. 1F, Supplemental Fig. S1G). We detected fewer WT1 positive cells on the surface of *Srsf3* cKO hearts compared to controls (Fig. 1F, G). It is important to note that ~90% of epicardial cells were tdTomato labelled in E12.5 control hearts, as Tg(Gata5-Cre) was not active in all epicardial progenitor cells. The proportion of epicardial cells positive for tdTomato was significantly decreased in *Srsf3* cKO compared to controls (Fig. 1H, Supplemental Fig. S1G), suggesting that non-targeted cells are either more proliferative or more likely to migrate onto the heart.

SRSF3 depletion in the PEO results in impaired proliferation and migration of epicardial progenitor cells

The impaired epicardial formation phenotype was confirmed in ventricular epicardial explants from E11.5 *Srsf3* cKO embryos, which demonstrated reduced outgrowth (Fig. 2A, B) and a lower proportion of tdTomato positive cells, compared with control (Fig. 2C). To assess if epicardial formation is disrupted from the outset, we checked for the presence of epicardial cells on the surface of the heart at E10.5, the stage when epicardial progenitor cells complete their migration. Few WT1 positive epicardial cells were detected in E10.5 *Srsf3* cKO hearts, in contrast to the extensive coverage attained in controls (Fig. 2D, Supplemental Fig. S2A). This prompted us to determine whether the formation of the proepicardium itself was impaired by loss of *Srsf3*. Indeed, we observed fewer epicardial progenitor cells in the PEO of *Srsf3* cKO embryos at E9.5 compared to controls (Fig. 2E), with mostly non-targeted cells remaining (white arrows). This was likely a consequence of impaired proliferation, as demonstrated by

bioRxiv preprint doi: https://doi.org/10.1101/2021.11.25.470003; this version posted November 25, 2021. The copyright holder for this preprint (which was not certified by peer review) is the author/funder, who has granted bioRxiv a license to display the preprint in perpetuity. It is made available under aCC-BY-NC-ND 4.0 International license.

diminished Ki67 expression (Supplemental Fig. S2B). To confirm this, PEO explants were cultured from control and *Srsf3* cKO embryos, and proliferation assessed (Fig. 2F - H, Supplemental Fig. S2C). As expected, *Srsf3*-depleted PEO explants were significantly smaller than controls (Fig. 2F, Supplemental Fig. S2C) and consisted of fewer Ki67 positive epicardial progenitor cells (Fig 2G, H), further supporting the notion that SRSF3 is required for proliferation of epicardial progenitor cells.

SRSF3 depletion in the epicardium leads to impaired proliferation and enhanced cell death in epicardial cells

To bypass the proepicardial defects and investigate SRSF3 function exclusively in the epicardium, we used the inducible Wt1CreERT2 line (Zhou et al. 2008; Xiao et al. 2018), with induction limited to E9.5 - E11.5 to avoid significant targeting of coronary endothelial cells (Lupu et al. 2020b). This strategy was adopted to generate an inducible Srsf3 KO (*Srsf3* iKO), with capacity to trace and temporally target the epicardial lineage (Fig. 3A). Embryonic hearts were first evaluated at E13.5, when the epicardium is fully formed and epiEMT has initiated in control embryos. While the epicardium formed in *Srsf3* iKO hearts, they exhibited a marked reduction in lineage-traced EPDCs (Fig. 3B), which coincided with impaired sprouting of vessels from the sinus venosus (Supplemental Fig. S3A), in keeping with the role of the epicardium in promoting coronary vessel growth (Lupu et al. 2020a). Since SRSF3 was required for proliferation of epicardial progenitors, we assessed Ki67 positive cells (Supplemental Fig. S3C - F). Epicardial explants cultured from E13.5 hearts revealed a mosaic loss of SRSF3, but, as expected, explants from Srsf3 iKO hearts contained fewer Ki67 positive cells (Supplemental Fig. S3D) due to loss of proliferation where *Srsf3* was successfully deleted (Supplemental Fig S3E, F). Impaired epiEMT and diminished emergence of EPDCs at E13.5 is consistent with the requirement of cell division for this process (Wu et al. 2010), further supporting the role of SRSF3 in epicardial proliferation.

We then examined the major transcriptional changes that occur in *Srsf3*-depleted epicardial cells at E13.5. Whole heart 10X chromium scRNA-seq was performed as opposed to bulk

bioRxiv preprint doi: https://doi.org/10.1101/2021.11.25.470003; this version posted November 25, 2021. The copyright holder for this preprint (which was not certified by peer review) is the author/funder, who has granted bioRxiv a license to display the preprint in perpetuity. It is made available under aCC-BY-NC-ND 4.0 International license.

RNA-seq since variable recombination was expected in individual epicardial cells (Fernandez-Chacon et al. 2019; Redpath and Smart 2021). Principal component analysis revealed 18 clusters, largely corresponding to discrete cardiomyocyte types, epicardial, mesenchymal, endocardial, and coronary endothelial cells (Fig. 3C, Supplemental Fig. S3G). The epicardial (Epi) cluster was identified based on mesothelial markers (Supplemental Fig. S3G), such as *Upk3b* (Kanamori-Katayama et al. 2011; Lupu et al. 2020b). The mesenchymal (Mes) cluster was derived from the epicardium, as indicated by widespread reporter expression (tdTomato; Supplemental Fig. S3H), thus essentially constituting EPDCs. Proportionally fewer mesenchymal cells were recovered in *Srsf3* iKO hearts in comparison to controls (Fig. 3C), supporting decreased EPDC formation. Next, we performed differential gene expression analysis guided by one clustering iteration of the Epi cluster in *Srsf3* iKO hearts. This resulted in three subsets: one cluster associated with proliferation genes (Epi_G2M) and two clusters associated with epicardial genes (Epi and Epi2) (Supplemental Fig. S3I). Notably, the Epi2 subset was enriched for genes associated with hypoxia, such as *Slc2a1* (Supplemental Fig. S3I), hypoxia-induced cell death, like *Fam162a*, and attenuated proliferation, such as *Ndrg1* (Fig. 3D, Supplemental Fig. S3I). The Epi2 cluster was not present in the control epicardium (Fig. 3D). Indeed, an upregulation in hypoxia-related genes was detected throughout *Srsf3* iKO hearts (Supplemental Fig. S3J), likely as a result of the coronary vessel defects. To validate the scRNA-seq data, fluorescence *in situ* hybridization (ISH) analysis showed upregulated *Ndrg1* in the epicardium of *Srsf3* iKO hearts (Fig. 3E), particularly at the apex where epiEMT hotspots were reported to be located (Sun et al. 2021). Increased frequency of TUNEL positive apoptotic epicardial cells (Fig. 3F, G) were observed in *Srsf3* iKO hearts compared to controls. The induction of apoptosis in *Srsf3* iKO but not *Srsf3* cKO epicardium suggests that SRSF3 depleted epicardial cells fail to cope with hypoxic stress and undergo cell death. Collectively, these data suggest that SRSF3 regulates epicardial proliferation and survival, to uphold epicardial function through EPDC contribution and promotion of coronary vessel growth.

bioRxiv preprint doi: https://doi.org/10.1101/2021.11.25.470003; this version posted November 25, 2021. The copyright holder for this preprint (which was not certified by peer review) is the author/funder, who has granted bioRxiv a license to display the preprint in perpetuity. It is made available under aCC-BY-NC-ND 4.0 International license.

SRSF3 regulates cell cycle progression in epicardial cells

To further investigate the role of SRSF3 in epicardial cell proliferation and avoid problems associated with *in vivo* administration of tamoxifen, the active form of tamoxifen, 4-OHT, was used to induce gene deletion *in vitro* in E11.5 epicardial explants (Fig. 4A). Direct treatment resulted in fewer epicardial cells (Fig. 4B) and smaller outgrowth (Fig. 4C) from *Srsf3* iKO explants compared to controls. While this strategy enabled more controlled targeting of cells, staining for SRSF3 still revealed mosaic depletion (Fig. 4D). In successfully targeted cells, (SRSF3-/lo), Ki67 expression was downregulated (Fig. 4D, E), reinforcing the finding that the proliferative capacity of SRSF3-depleted epicardial cells is impaired.

We next utilised a mouse epicardial cell line (Austin et al. 2008) to knock-down SRSF3 using a Cre-independent strategy: RNA interference (Fig. 4F, Supplemental Fig. S4A). To further explore the mechanisms underlying decreased proliferation in SRSF3-depleted epicardial cells, we assessed cyclin D1 (CCND1) expression. CCND1 is a known target of SRSF3 and is required for cell cycle progression (Kurokawa et al. 2013). Immunostaining revealed a significant reduction of cells positive for CCND1 in siSRSF3 transfected epicardial cells (Fig. 4G), further supporting that SRSF3 is required for production of CCND1 protein. Together, these results suggest depletion of SRSF3 in epicardial cells induces cell cycle arrest.

Non-recombined epicardial lineage cells compensate for loss of SRSF3-depleted cells

Having identified defects in epicardial activity at E13.5 due to SRSF3 loss, such as impaired proliferation and increased cell death, we next assessed *Srsf3* iKO hearts at E15.5, using SMART-Seq2 (Picelli et al. 2014) of tdTomato positive FACS sorted cells. At E15.5, the epicardial lineage in *Srsf3* iKO hearts displayed similar composition to controls, consisting of a small epicardial cluster, two mesenchymal clusters, and a distinct cluster of mural cells (Fig. 5A, Supplemental Fig. S5A). We previously characterised Mes1 as subepicardial mesenchyme and Mes2 as fibroblast-like cells (Lupu et al. 2020b). Since the plate-based SMART-Seq2 method allows recovery of full-length mRNA, we could establish that cells lacking *Srsf3* exons 2/3 were absent at this stage, indicating that *Srsf3*-depleted cells were

bioRxiv preprint doi: https://doi.org/10.1101/2021.11.25.470003; this version posted November 25, 2021. The copyright holder for this preprint (which was not certified by peer review) is the author/funder, who has granted bioRxiv a license to display the preprint in perpetuity. It is made available under aCC-BY-NC-ND 4.0 International license.

lost earlier in development. To confirm that only non-recombined cells remained, E15.5 explants were stained for SRSF3 (Supplemental Fig. S5B). All cells in the E15.5 epicardial explants had high levels of SRSF3, confirming that the SRSF3-depleted cells had been removed earlier in development. Surprisingly, the SMART-Seq2 data actually indicated increased *Srsf3* expression in the *Srsf3* iKO hearts in both epicardial and subepicardial mesenchymal cells, which was confirmed by SRSF3 IHC (Fig. 5B, C, Supplemental Fig. S5C). The increased SRSF3 expression coincided with increased proliferation, as indicated by *Top2a* expression and confirmed by TOP2A staining. (Fig. 5D, E, Supplemental Fig. S5D). We found that the reduced incidence of EPDCs invading the myocardium at E13.5 through to E15.5 (Fig. 5F, Supplemental Fig. S5E) was fully restored by E17.5 (Fig. 5G, Supplemental Fig. S5E), with hearts appearing morphologically normal (Supplemental Fig. S5F). Together, these data indicate that non-recombined epicardial cells compensate for the early loss of SRSF3-depleted cells, by using SRSF3-controlled mechanisms to promote epicardial proliferation and restore normal function.

SRSF3 depletion in epicardial progenitors leads to compaction and coronary vasculature defects

To explore more severe defects and the extent to which compensatory mechanisms could overcome early epicardial deficiencies (Supplementary Fig. S6A), we tested two strategies to achieve more efficient gene deletion in the *Srsf3* iKO model with a higher dose of tamoxifen (80mg/kg): at i) E8.5, expected to target progenitors in the PEO; ii) E9.5, expected to improve targeting of epicardial founders. We observed that induction at E8.5 resulted in myocardial non-compaction, as revealed by the persistence of a highly trabeculated endocardium (EMCN+) at E17.5, which extended closer to the epicardial surface (Fig. 6A). Moreover, superficial vessels were more numerous in *Srsf3* iKO hearts compared to littermate controls (Fig. 6A; arrows).In contrast, Srsf3 iKO hearts appeared normal when tamoxifen was administered at E9.5, similar to the E9.5/E11.5 phenotype (Fig. 6A) and presumably achieved by the SRSF3-dependent compensatory mechanisms described above. Impaired coronary

bioRxiv preprint doi: https://doi.org/10.1101/2021.11.25.470003; this version posted November 25, 2021. The copyright holder for this preprint (which was not certified by peer review) is the author/funder, who has granted bioRxiv a license to display the preprint in perpetuity. It is made available under aCC-BY-NC-ND 4.0 International license.

vasculature formation, appearance of ectopic subepicardial vessels and myocardial non-compaction are defects frequently reported in hearts with compromised epicardial function (Smart et al. 2007; Phillips et al. 2008; Tian et al. 2013). Taken together, these data indicate that the transient functional impairments observed with the original tamoxifen regime persist when a higher efficiency SRSF3 depletion is achieved (Fig. 6A, Supplemental Fig. S6B), due to the essential role of cell division in epicardial function (Wu et al. 2010).

Discussion

Our study presents insight into the critical role of SRSF3 in the (pro)epicardium, particularly mediating proliferation during heart development. We show that SRSF3 expression is widespread in embryonic hearts, with highest levels detected in proepicardial cells and in the epicardial layer until E12.5. Constitutive SRSF3 depletion in epicardial progenitor cells resulted in gross morphological heart abnormalities and embryonic lethality at E12.5. Failure to form the epicardial layer was due to a diminished source of epicardial progenitor cells within the PEO, as a result of their decreased proliferative capacity in the absence of SRSF3. However, recombination in the Tg(Gata5-Cre) model also targeted a subset of cardiomyocytes, thus, combined depletion of SRSF3, in most epicardial progenitor cells and a subset of cardiomyocytes, contributed to the severe phenotype, as embryos with impaired epicardial formation generally die at later stages (von Gise et al. 2011; Li et al. 2017). Early stage embryonic lethality was previously reported in cardiac-specific SRSF3 knockout mice due to impaired cardiomyocyte proliferation and survival (Ortiz-Sánchez et al. 2019).

Notably, peak epicardial SRSF3 expression at E11.5 coincides with the reported peak of proliferative activity (Wu et al. 2010). Temporal induction and selective deletion of SRSF3 in epicardial cells, using the Wt1CreERT2 line, resulted in impaired proliferation, ultimately leading to loss of SRSF3-depleted epicardial cells from the heart. SRSF3 was key to epicardial cell cycle progression as SRSF3-depleted cells *in vitro* downregulated expression of cyclin D1. This is consistent with the role of SRSF3 as a positive regulator of G1 to S phase transition,

bioRxiv preprint doi: https://doi.org/10.1101/2021.11.25.470003; this version posted November 25, 2021. The copyright holder for this preprint (which was not certified by peer review) is the author/funder, who has granted bioRxiv a license to display the preprint in perpetuity. It is made available under aCC-BY-NC-ND 4.0 International license.

via stimulation of cyclins (Kano et al. 2013; Kurokawa et al. 2013). Moreover, SRSF3 depletion upregulated *Ndrg1* expression in the epicardium, a gene which was formerly identified to stimulate G1 phase cell cycle arrest in tumour cells (Akiba et al. 2011). Reinforcing the notion that SRSF3 critically drives cell cycle in the epicardium, a noteable finding was that epicardial cells which escaped recombination were able to hyper-proliferate and restore epicardial function, in part, by over-expressing SRSF3.

SRSF3 depletion in the epicardium resulted in cell death typically associated with hypoxic stress, exemplified by upregulated *Fam162a* and increase in TUNEL+ epicardial cells. *Fam162a* is a transcriptional target of HIF-1α, to promote its expression under hypoxic conditions (Lee et al. 2004). It is probable that delayed sinus venosus sprouting in *Srsf3* iKO hearts causes hypoxic stress. A limitation of our study, in this regard, is that we cannot distinguish whether SRSF3 directly regulates *Fam162a*, or whether upregulation is simply a consequence of impaired vascular development. Interestingly, acute hypoxia in tilapia fish resulted in alternative splicing of *Fam162a* (Xia et al. 2018). In cancer, de-regulated expression of RNA splicing factors such as SRSF3, were reported to mediate numerous alternative splicing events to promote evasion of apoptosis (Farina et al. 2020). Either way, SRSF3 depletion may expose epicardial cells to hypoxia-induced apoptosis, and the relationship between SRSF3 and *Fam162a* warrants further investigation.

Induction of SRSF3 deletion using the Wt1CreERT2 at E8.5 did not result in failure of the epicardium to form, unlike Tg(Gata5-Cre) targeting. This could be due either to the reduced efficiency of the inducible Cre or the timing of Cre activation, at the onset of proepicardial formation with Tg(Gata5-Cre) and a considerable lag between tamoxifen delivery and recombination in the case of Wt1CreERT2 (Hayashi and McMahon 2002). Although the epicardial layer was established in Srsf3 iKO hearts, epicardial function was clearly defective, manifested as myocardial non-compaction and impaired coronary vessel formation, consistent

bioRxiv preprint doi: https://doi.org/10.1101/2021.11.25.470003; this version posted November 25, 2021. The copyright holder for this preprint (which was not certified by peer review) is the author/funder, who has granted bioRxiv a license to display the preprint in perpetuity. It is made available under aCC-BY-NC-ND 4.0 International license.

with other studies (Smart et al. 2007; Martínez-Estrada et al. 2010; von Gise et al. 2011; Tian et al. 2013). In contrast, induction of SRSF3 depletion at E9.5 or E9.5/ E11.5 resulted in normal heart morphology at E17.5 due to the ability of non-recombined cells to over-express SRSF3 and "hyperproliferation" to restore the epicardial lineage. The compensation mechanism is probably facilitated by the loss of SRSF3-depleted cells and by cell competition mechanisms that are active in the epicardium, as previously demonstrated with overexpression of c-MYC (Villa Del Campo et al. 2016). c-MYC overexpressing cells similarly become hyperproliferative and out-compete wild-type cells in epicardial explants (Villa Del Campo et al. 2016). Alternatively, hypoxic stress generated by diminished SV sprouting may upregulate SRSF3 in non-recombined cells, in line with reported hypoxia-induced SRSF3 expression (Brady et al. 2017), to enhance their proliferation. Thus, this study reveals an extraordinary potential of epicardial cells to hyperproliferate and compensate in the presence of genetic changes. It also highlights the limitations of variable recombination efficiency which may confound investigation of critical genes in the maturing epicardium.

Our study adds to current literature describing the key role of SRSF3 in cellular proliferation (Gonçalves et al. 2009; Änkö et al. 2010; Jia et al. 2010; Corbo et al. 2013; Kano et al. 2013; Kurokawa et al. 2013; Ajiro et al. 2016). In the context of cardiac development, SRSF3 is required for the proliferation and survival of (pro)epicardial cells. SRSF3 regulation of cell cycle progression is essential to enable epicardial cells to undergo epiEMT and to subsequently support vascular development. This study defines SRSF3 as a key regulator of epicardial cell behaviour during development. Moreover, the finding that compensatory restoration of the epicardium can be achieved by induction of cell cycling may provide relevant insights for regenerative therapies.

Materials and methods

Mouse strains

bioRxiv preprint doi: https://doi.org/10.1101/2021.11.25.470003; this version posted November 25, 2021. The copyright holder for this preprint (which was not certified by peer review) is the author/funder, who has granted bioRxiv a license to display the preprint in perpetuity. It is made available under aCC-BY-NC-ND 4.0 International license.

Conditional and inducible targeting of SRSF3 was achieved by crossing epicardial Cre lines. Tg(Gata5-Cre) (Merki et al. 2005) and Wt1CreERT2 (Zhou et al. 2008), respectively, with mice in which exons 2 and 3 of *Srsf3* were flanked by loxP sites (Ortiz-Sánchez et al. 2019). The epicardial lineage was traced using Rosa26tdTomato (Madisen et al. 2010). Pregnant females were oral gavaged with 40mg/kg at E9.5 and E11.5, or 80mg/kg tamoxifen at E8.5 or E9.5 (where specifically stated). All procedures were approved by the University of Oxford Animal Welfare and Ethical Review Board, in accordance with Animals (Scientific Procedures) Act 1986 (Home Office, UK).

Tissue harvest and cryosections

Embryos and embryonic hearts were harvested and fixed in 4% PFA for 2h at room temperature (RT). Following PBS washes, tissues were equilibrated overnight at 4°C in 30% sucrose/PBS, and then gradually transitioned into O.C.T. Samples were stored at -80°C, then cryosectioned at 8-12µm thickness.

(Pro)epicardial explant and cell line culture

Embryonic hearts were dissected into atrial and ventricular pieces and cultured on 1% gelatine in culture medium (15% FBS, 1% Penicillin/Streptomycin, DMEM high glucose Glutamax). Explants were incubated at 37°C in 5% CO_2 for 3 days. Dissected proepicardia were subjected to the same culture conditions as above. The strategy to induce SRSF3 depletion *in vitro* involved culturing epicardial explants in culture medium supplemented with 1µM 4-Hydroxytamoxifen (4-OHT). An immortalised epicardium-derived cell line (Austin et al. 2008) was cultured on 1% gelatine in immorto medium (10% FBS, 1% Penicillin/Streptomycin, ITS supplement, 0.1% INFγ, DMEM high glucose Glutamax) at 33°C in 5% CO_2. Cells were transfected with 40nM siRNA (siControl; silencer siRNA negative control Cat. #4390843, siSrsf3 #1; s73613, siSrsf3 #2; s73615, ThermoFisher) for 48h at 33°C using Lipofectamine RNAiMAX Transfection Procedure (ThermoFisher Cat.#13778-100).

Immunofluorescence

bioRxiv preprint doi: https://doi.org/10.1101/2021.11.25.470003; this version posted November 25, 2021. The copyright holder for this preprint (which was not certified by peer review) is the author/funder, who has granted bioRxiv a license to display the preprint in perpetuity. It is made available under aCC-BY-NC-ND 4.0 International license.

Cryosections were subjected to a standard immunofluorescence protocol detailed in Supplemental Methods. Cultured explants and cell line were subjected to the same immunofluorescence protocol, but without the initial permeabilization (0.5% TX) step. Images were acquired using Leica DM6000 fluorescence microscope or Olympus Fluoview-1000 confocal microscope and processed using Fiji software. Quantification was carried out in Fiji or CellProfiler software.

RNA extraction and qRT-PCR

RNA was extracted from embryonic hearts using RNeasy Mini kit (Qiagen) according to the manufacturer's instructions. cDNA was prepared with High-Capacity cDNA Reverse Transcription kit (ThermoFisher) according to the manufacturer's instructions and analysed by quantitative RT-PCR using the Fast SYBR Green Master Mix (ThermoFisher). Primers are listed in the Supplemental Methods Table S2.

Flow cytometry

Enzymatically dissociated hearts were stained for cell viability, and immunostained for CD31 and cTNT as previously described (Lupu et al. 2020b; Redpath et al. 2021). Viability stains and antibodies are listed in the Supplemental Methods Table S1. Samples were processed on BD LSRFORTESSA X-20 cytometer and analysed using FlowJo software.

Single-cell RNA-sequencing and analysis

E13.5 heart and E15.5 ventricles were enzymatically dissociated and prepared for scRNA-seq as previously described (Lupu et al. 2020b; Redpath et al. 2021). E13.5 samples were used in Chromium 10X system. E15.5 samples were FACS-sorted for live epicardial lineage cells (tdTomato+) and subjected to plate-based Smart-Seq2 protocol, as described for the previously published control samples (Lupu et al. 2020b). Library preparation and sequencing details are provided in Supplemental Material. All scRNA-seq datasets were analysed using Seurat (Butler et al. 2018; Stuart et al. 2019) in R as follows: principal component analysis was used to cluster cells, which were visualised with the UMAP method (Becht et al. 2018;

bioRxiv preprint doi: https://doi.org/10.1101/2021.11.25.470003; this version posted November 25, 2021. The copyright holder for this preprint (which was not certified by peer review) is the author/funder, who has granted bioRxiv a license to display the preprint in perpetuity. It is made available under aCC-BY-NC-ND 4.0 International license.

Butler et al. 2018) and biological samples – control and Srsf3 iKO hearts – integrated using CCA- based Seurat Integration.

Fluorescence in situ hybridization (mRNA)

RNAscope Multiplex Fluorescent v2 assay (ACD) was performed on cryosections according to manufacturer's instructions, with minor modifications as previously described (Lupu et al. 2020b). Ndrg1 and negative control probe, and TSA plus fluorophores are listed in Supplemental Methods Table S3.

TUNEL assay

Click-iT™ Plus TUNEL Assay (ThermoFisher) was performed on cryosections according to the manufacturer's instructions.

Data access

All sequencing data from this study are available in Gene Expression Omnibus database under accession number GSE145832 and TBC.

Detailed protocols provided in Supplemental Methods.

Competing interest statement

The authors declare no competing interests.

Acknowledgements

We thank Prof Peter Nielsen, Max Planck Institute, and Prof Enrique Lara-Pezzi, CNIC, for the Srsf3$^{fl/fl}$ line; Prof William Pu, Harvard, for the Wt1CreERT2 line; Dr Madeleine Lemieux (Bioinfo) for processing SMART-Seq2 and 10X data; Dr Neil Ashley, WIMM Single cell facility, for sequencing, the Dunn School Flow Cytometry facility for equipment use, Micron for microscopy facilities and Biomedical Services staff for animal husbandry. This work was funded by the British Heart Foundation (BHF): DPhil Studentship (FS/15/68/32042); BHF Project grant (PG/15/112/31940); BHF Ian Fleming Senior Basic Science Research

bioRxiv preprint doi: https://doi.org/10.1101/2021.11.25.470003; this version posted November 25, 2021. The copyright holder for this preprint (which was not certified by peer review) is the author/funder, who has granted bioRxiv a license to display the preprint in perpetuity. It is made available under aCC-BY-NC-ND 4.0 International license.

Fellowships (FS/13/4/30045 and FS/19/32/34376); BHF Centre of Regenerative Medicine, Oxbridge (RM/13/3/30159).

Author contributions

Conceptualisation, I-EL, NS; Methodology, I-EL; Investigation, I-EL, ANR; Formal Analysis, I-EL, ANR, NS; Visualisation, I-EL, ANR; Writing – Original Draft, I-EL, ANR; Writing – Review and Editing, I-EL, ANR, NS; Funding Acquisition, NS; Supervision, ANR and NS.

References

Ajiro M, Jia R, Yang Y, Zhu J, Zheng Z-M. 2016. A genome landscape of SRSF3-regulated splicing events and gene expression in human osteosarcoma U2OS cells. *Nucleic Acids Res* **44**: 1854-1870.

Akiba J, Murakami Y, Noda M, Watari K, Ogasawara S, Yoshida T, Kawahara A, Sanada S, Yasumoto M, Yamaguchi R et al. 2011. N-myc downstream regulated gene1/Cap43 overexpression suppresses tumor growth by hepatic cancer cells through cell cycle arrest at the G0/G1 phase. *Cancer Lett* **310**: 25-34.

Andrés-Delgado L, Ernst A, Galardi-Castilla M, Bazaga D, Peralta M, Münch J, González-Rosa JM, Marques I, Tessadori F, de la Pompa JL et al. 2019. Actin dynamics and the Bmp pathway drive apical extrusion of proepicardial cells. *Development* **146**: dev174961.

Änkö M-L, Morales L, Henry I, Beyer A, Neugebauer KM. 2010. Global analysis reveals SRp20- and SRp75-specific mRNPs in cycling and neural cells. *Nature Structural & Molecular Biology* **17**: 962-970.

Änkö M-L, Müller-McNicoll M, Brandl H, Curk T, Gorup C, Henry I, Ule J, Neugebauer KM. 2012. The RNA-binding landscapes of two SR proteins reveal unique functions and binding to diverse RNA classes. *Genome Biol* **13**: R17-R17.

Austin AF, Compton LA, Love JD, Brown CB, Barnett JV. 2008. Primary and immortalized mouse epicardial cells undergo differentiation in response to TGFβ. *Developmental Dynamics* **237**: 366-376.

Baek ST, Tallquist MD. 2012. Nf1 limits epicardial derivative expansion by regulating epithelial to mesenchymal transition and proliferation. *Development* **139**: 2040-2049.

Becht E, Dutertre C-A, Kwok IWH, Ng LG, Ginhoux F, Newell EW. 2018. Evaluation of UMAP as an alternative to t-SNE for single-cell data. Cold Spring Harbor Laboratory.

Brady LK, Wang H, Radens CM, Bi Y, Radovich M, Maity A, Ivan C, Ivan M, Barash Y, Koumenis C. 2017. Transcriptome analysis of hypoxic cancer cells uncovers intron retention in EIF2B5 as a mechanism to inhibit translation. *PLoS Biol* **15**: e2002623.

Butler A, Hoffman P, Smibert P, Papalexi E, Satija R. 2018. Integrating single-cell transcriptomic data across different conditions, technologies, and species. *Nat Biotechnol* **36**: 411-420.

Cao J, Navis A, Cox BD, Dickson AL, Gemberling M, Karra R, Bagnat M, Poss KD. 2016. Single epicardial cell transcriptome sequencing identifies Caveolin 1 as an essential factor in zebrafish heart regeneration. *Development* **143**: 232-243.

Cao Y, Cao J. 2018. Covering and Re-Covering the Heart: Development and Regeneration of the Epicardium. *J Cardiovasc Dev Dis* **6**: 3.

Corbo C, Orrù S, Salvatore F. 2013. SRp20: An overview of its role in human diseases. *Biochemical and Biophysical Research Communications* **436**: 1-5.

Do DV, Strauss B, Cukuroglu E, Macaulay I, Wee KB, Hu TX, Igor RDLM, Lee C, Harrison A, Butler R et al. 2018. SRSF3 maintains transcriptome integrity in oocytes by regulation of alternative splicing and transposable elements. *Cell Discov* **4**: 33-33.

Dubé KN, Thomas TM, Munshaw S, Rohling M, Riley PR, Smart N. 2017. Recapitulation of developmental mechanisms to revascularize the ischemic heart. *JCI Insight* **2**: e96800.

bioRxiv preprint doi: https://doi.org/10.1101/2021.11.25.470003; this version posted November 25, 2021. The copyright holder for this preprint (which was not certified by peer review) is the author/funder, who has granted bioRxiv a license to display the preprint in perpetuity. It is made available under aCC-BY-NC-ND 4.0 International license.

Farina AR, Cappabianca L, Sebastiano M, Zelli V, Guadagni S, Mackay AR. 2020. Hypoxia-induced alternative splicing: the 11th Hallmark of Cancer. *J Exp Clin Cancer Res* **39**: 110.

Fernandez-Chacon M, Casquero-Garcia V, Luo W, Lunella FF, Rocha SF, Del Olmo-Cabrera S, Benedito R. 2019. iSuRe-Cre is a genetic tool to reliably induce and report Cre-dependent genetic modifications. *Nat Commun* **10**.

Gonçalves V, Matos P, Jordan P. 2009. Antagonistic SR proteins regulate alternative splicing of tumor-related Rac1b downstream of the PI3-kinase and Wnt pathways. *Human Molecular Genetics* **18**: 3696-3707.

Hayashi S, McMahon AP. 2002. Efficient Recombination in Diverse Tissues by a Tamoxifen-Inducible Form of Cre: A Tool for Temporally Regulated Gene Activation/Inactivation in the Mouse. *Developmental Biology* **244**: 305-318.

Jia R, Li C, McCoy JP, Deng C-X, Zheng Z-M. 2010. SRp20 is a proto-oncogene critical for cell proliferation and tumor induction and maintenance. *Int J Biol Sci* **6**: 806-826.

Jumaa H, Wei G, Nielsen PJ. 1999. Blastocyst formation is blocked in mouse embryos lacking the splicing factor SRp20. *Current Biology* **9**: 899-902.

Kanamori-Katayama M, Kaiho A, Ishizu Y, Okamura-Oho Y, Hino O, Abe M, Kishimoto T, Sekihara H, Nakamura Y, Suzuki H et al. 2011. LRRN4 and UPK3B are markers of primary mesothelial cells. *PLoS One* **6**: e25391-e25391.

Kano S, Nishida K, Nishiyama C, Akaike Y, Kajita K, Kurokawa K, Masuda K, Kuwano Y, Tanahashi T, Rokutan K. 2013. Truncated serine/arginine-rich splicing factor 3 accelerates cell growth through up-regulating c-Jun expression. *The Journal of Medical Investigation* **60**: 228-235.

Ke H, Zhao L, Zhang H, Feng X, Xu H, Hao J, Wang S, Yang Q, Zou L, Su X et al. 2018. Loss of TDP43 inhibits progression of triple-negative breast cancer in coordination with SRSF3. *Proc Natl Acad Sci U S A* **115**: E3426-E3435.

Kikuchi K, Gupta V, Wang J, Holdway JE, Wills AA, Fang Y, Poss KD. 2011. tcf21+ epicardial cells adopt non-myocardial fates during zebrafish heart development and regeneration. *Development* **138**: 2895-2902.

Kim HR, Hwang SJ, Shin CH, Choi KH, Ohn T, Kim HH. 2017. SRSF3-regulated miR-132/212 controls cell migration and invasion by targeting YAP1. *Experimental Cell Research* **358**: 161-170.

Kim J, Park RY, Chen JK, Kim J, Jeong S, Ohn T. 2014. Splicing factor SRSF3 represses the translation of programmed cell death 4 mRNA by associating with the 5'-UTR region. *Cell Death Differ* **21**: 481-490.

Kurokawa K, Akaike Y, Masuda K, Kuwano Y, Nishida K, Yamagishi N, Kajita K, Tanahashi T, Rokutan K. 2013. Downregulation of serine/arginine-rich splicing factor 3 induces G1 cell cycle arrest and apoptosis in colon cancer cells. *Oncogene* **33**: 1407-1417.

Lee MJ, Kim JY, Suk K, Park JH. 2004. Identification of the hypoxia-inducible factor 1 alpha-responsive HGTD-P gene as a mediator in the mitochondrial apoptotic pathway. *Mol Cell Biol* **24**: 3918-3927.

Lepilina A, Coon AN, Kikuchi K, Holdway JE, Roberts RW, Burns CG, Poss KD. 2006. A Dynamic Epicardial Injury Response Supports Progenitor Cell Activity during Zebrafish Heart Regeneration. *Cell* **127**: 607-619.

Li J, Miao L, Zhao C, Shaikh Qureshi WM, Shieh D, Guo H, Lu Y, Hu S, Huang A, Zhang L et al. 2017. CDC42 is required for epicardial and pro-epicardial development by mediating FGF receptor trafficking to the plasma membrane. *Development* **144**: 1635-1647.

Liu Q, Zhang H, Tian X, He L, Huang X, Tan Z, Yan Y, Evans SM, Wythe JD, Zhou B. 2016. Smooth muscle origin of postnatal 2nd CVP is pre-determined in early embryo. *Biochemical and biophysical research communications* **471**: 430-436.

Lupu IE, De Val S, Smart N. 2020a. Coronary vessel formation in development and disease: mechanisms and insights for therapy. *Nat Rev Cardiol* **17**: 790-806.

Lupu IE, Redpath AN, Smart N. 2020b. Spatiotemporal Analysis Reveals Overlap of Key Proepicardial Markers in the Developing Murine Heart. *Stem Cell Reports* **14**: 770-787.

Madisen L, Zwingman TA, Sunkin SM, Oh SW, Zariwala HA, Gu H, Ng LL, Palmiter RD, Hawrylycz MJ, Jones AR et al. 2010. A robust and high-throughput Cre reporting and characterization system for the whole mouse brain. *Nat Neurosci* **13**: 133-140.

Martínez-Estrada OM, Lettice LA, Essafi A, Guadix JA, Slight J, Velecela V, Hall E, Reichmann J, Devenney PS, Hohenstein P et al. 2010. Wt1 is required for cardiovascular progenitor cell formation through transcriptional control of Snail and E-cadherin. *Nat Genet* **42**: 89-93.

Mellgren AM, Smith CL, Olsen GS, Eskiocak B, Zhou B, Kazi MN, Ruiz FR, Pu WT, Tallquist MD. 2008. Platelet-derived growth factor receptor beta signaling is required for efficient epicardial cell

bioRxiv preprint doi: https://doi.org/10.1101/2021.11.25.470003; this version posted November 25, 2021. The copyright holder for this preprint (which was not certified by peer review) is the author/funder, who has granted bioRxiv a license to display the preprint in perpetuity. It is made available under aCC-BY-NC-ND 4.0 International license.

migration and development of two distinct coronary vascular smooth muscle cell populations. *Circulation research* **103**: 1393-1401.

Merki E, Zamora M, Raya A, Kawakami Y, Wang J, Zhang X, Burch J, Kubalak SW, Kaliman P, Izpisua Belmonte JC et al. 2005. Epicardial retinoid X receptor alpha is required for myocardial growth and coronary artery formation. *Proc Natl Acad Sci U S A* **102**: 18455-18460.

Müller-McNicoll M, Botti V, de Jesus Domingues AM, Brandl H, Schwich OD, Steiner MC, Curk T, Poser I, Zarnack K, Neugebauer KM. 2016. SR proteins are NXF1 adaptors that link alternative RNA processing to mRNA export. *Genes & development* **30**: 553-566.

Mure F, Corbin A, Benbahouche NEH, Bertrand E, Manet E, Gruffat H. 2018. The splicing factor SRSF3 is functionally connected to the nuclear RNA exosome for intronless mRNA decay. *Sci Rep* **8**: 12901-12901.

Ortiz-Sánchez P, Villalba-Orero M, López-Olañeta MM, Larrasa-Alonso J, Sánchez-Cabo F, Martí-Gómez C, Camafeita E, Gómez-Salinero JM, Ramos-Hernández L, Nielsen PJ et al. 2019. Loss of SRSF3 in Cardiomyocytes Leads to Decapping of Contraction-Related mRNAs and Severe Systolic Dysfunction. *Circulation research* **125**: 170-183.

Park SK, Jeong S. 2016. SRSF3 represses the expression of PDCD4 protein by coordinated regulation of alternative splicing, export and translation. *Biochemical and Biophysical Research Communications* **470**: 431-438.

Phillips HM, Hildreth V, Peat JD, Murdoch JN, Kobayashi K, Chaudhry B, Henderson DJ. 2008. Non-cell-autonomous roles for the planar cell polarity gene Vangl2 in development of the coronary circulation. *Circulation Research* **102**: 615-623.

Picelli S, Faridani OR, Björklund ÅK, Winberg G, Sagasser S, Sandberg R. 2014. Full-length RNA-seq from single cells using Smart-seq2. *Nature Protocols* **9**: 171-181.

Ratnadiwakara M, Archer SK, Dent CI, Ruiz De Los Mozos I, Beilharz TH, Knaupp AS, Nefzger CM, Polo JM, Anko M-L. 2018. SRSF3 promotes pluripotency through Nanog mRNA export and coordination of the pluripotency gene expression program. *Elife* **7**: e37419.

Redpath AN, Lupu IE, Smart N. 2021. Analysis of epicardial genes in embryonic mouse hearts with flow cytometry. *STAR Protoc* **2**: 100359.

Redpath AN, Smart N. 2021. Recapturing embryonic potential in the adult epicardium: Prospects for cardiac repair. *Stem Cells Transl Med* **10**: 511-521.

Rudat C, Norden J, Taketo MM, Kispert A. 2013. Epicardial function of canonical Wnt-, Hedgehog-, Fgfr1/2-, and Pdgfra-signalling. *Cardiovascular Research* **100**: 411-421.

Schulte I, Schlueter J, Abu-Issa R, Brand T, Männer J. 2007. Morphological and molecular left–right asymmetries in the development of the proepicardium: A comparative analysis on mouse and chick embryos. *Developmental Dynamics* **236**: 684-695.

Sen S, Jumaa H, Webster NJG. 2013. Splicing factor SRSF3 is crucial for hepatocyte differentiation and metabolic function. *Nat Commun* **4**: 1336-1336.

Sen S, Langiewicz M, Jumaa H, Webster NJG. 2015. Deletion of serine/arginine-rich splicing factor 3 in hepatocytes predisposes to hepatocellular carcinoma in mice. *Hepatology* **61**: 171-183.

Shen H, Kan JLC, Green MR. 2004. Arginine-Serine-Rich Domains Bound at Splicing Enhancers Contact the Branchpoint to Promote Prespliceosome Assembly. *Molecular Cell* **13**: 367-376.

Shepard PJ, Hertel KJ. 2009. The SR protein family. *Genome Biol* **10**: 242-242.

Singh A, Ramesh S, Cibi DM, Yun LS, Li J, Li L, Manderfield LJ, Olson EN, Epstein JA, Singh MK. 2016. Hippo Signaling Mediators Yap and Taz Are Required in the Epicardium for Coronary Vasculature Development. *Cell Rep* **15**: 1384-1393.

Smart N, Riley PR. 2012. The epicardium as a candidate for heart regeneration. *Future Cardiol* **8**: 53-69.

Smart N, Risebro CA, Melville AAD, Moses K, Schwartz RJ, Chien KR, Riley PR. 2007. Thymosin beta-4 Is Essential for Coronary Vessel Development and Promotes Neovascularization via Adult Epicardium. *Annals of the New York Academy of Sciences* **1112**: 171-188.

Smith CL, Baek ST, Sung CY, Tallquist MD. 2011. Epicardial-derived cell epithelial-to-mesenchymal transition and fate specification require PDGF receptor signaling. *Circulation research* **108**: e15-e26.

Stuart T, Butler A, Hoffman P, Hafemeister C, Papalexi E, Mauck WM, 3rd, Hao Y, Stoeckius M, Smibert P, Satija R. 2019. Comprehensive Integration of Single-Cell Data. *Cell* **177**: 1888-1902 e1821.

Sun X, Malandraki-Miller S, Kennedy T, Bassat E, Klaourakis K, Zhao J, Gamen E, Vieira JM, Tzahor E, Riley PR. 2021. The extracellular matrix protein agrin is essential for epicardial epithelial-to-mesenchymal transition during heart development. *Development* **148**.

bioRxiv preprint doi: https://doi.org/10.1101/2021.11.25.470003; this version posted November 25, 2021. The copyright holder for this preprint (which was not certified by peer review) is the author/funder, who has granted bioRxiv a license to display the preprint in perpetuity. It is made available under aCC-BY-NC-ND 4.0 International license.

Tang Y, Horikawa I, Ajiro M, Robles AI, Fujita K, Mondal AM, Stauffer JK, Zheng ZM, Harris CC. 2013. Downregulation of splicing factor SRSF3 induces p53β, an alternatively spliced isoform of p53 that promotes cellular senescence. *Oncogene* **32**: 2792-2798.

Tian X, Hu T, Zhang H, He L, Huang X, Liu Q, Yu W, He L, Yang Z, Zhang Z et al. 2013. Subepicardial endothelial cells invade the embryonic ventricle wall to form coronary arteries. *Cell Res* **23**: 1075-1090.

Vieira JM, Howard S, Villa Del Campo C, Bollini S, Dube KN, Masters M, Barnette DN, Rohling M, Sun X, Hankins LE et al. 2017. BRG1-SWI/SNF-dependent regulation of the Wt1 transcriptional landscape mediates epicardial activity during heart development and disease. *Nat Commun* **8**: 16034.

Villa Del Campo C, Lioux G, Carmona R, Sierra R, Muñoz-Chápuli R, Clavería C, Torres M. 2016. Myc overexpression enhances of epicardial contribution to the developing heart and promotes extensive expansion of the cardiomyocyte population. *Sci Rep* **6**: 35366-35366.

von Gise A, Zhou B, Honor LB, Ma Q, Petryk A, Pu WT. 2011. WT1 regulates epicardial epithelial to mesenchymal transition through β-catenin and retinoic acid signaling pathways. *Developmental biology* **356**: 421-431.

Wang J, Cao J, Dickson AL, Poss KD. 2015. Epicardial regeneration is guided by cardiac outflow tract and Hedgehog signalling. *Nature* **522**: 226-230.

Wu M, Smith CL, Hall JA, Lee I, Luby-Phelps K, Tallquist MD. 2010. Epicardial spindle orientation controls cell entry into the myocardium. *Dev Cell* **19**: 114-125.

Xia JH, Li HL, Li BJ, Gu XH, Lin HR. 2018. Acute hypoxia stress induced abundant differential expression genes and alternative splicing events in heart of tilapia. *Gene* **639**: 52-61.

Xiao Y, Hill MC, Zhang M, Martin TJ, Morikawa Y, Wang S, Moise AR, Wythe JD, Martin JF. 2018. Hippo Signaling Plays an Essential Role in Cell State Transitions during Cardiac Fibroblast Development. *Dev Cell* **45**: 153-169.e156.

Zahler AM, Lane WS, Stolk JA, Roth MB. 1992. SR proteins: a conserved family of pre-mRNA splicing factors. *Genes & Development* **6**: 837-847.

Zhou B, Ma Q, Rajagopal S, Wu SM, Domian I, Rivera-Feliciano J, Jiang D, von Gise A, Ikeda S, Chien KR et al. 2008. Epicardial progenitors contribute to the cardiomyocyte lineage in the developing heart. *Nature* **454**: 109-113.

bioRxiv preprint doi: https://doi.org/10.1101/2021.11.25.470003; this version posted November 25, 2021. The copyright holder for this preprint (which was not certified by peer review) is the author/funder, who has granted bioRxiv a license to display the preprint in perpetuity. It is made available under aCC-BY-NC-ND 4.0 International license.

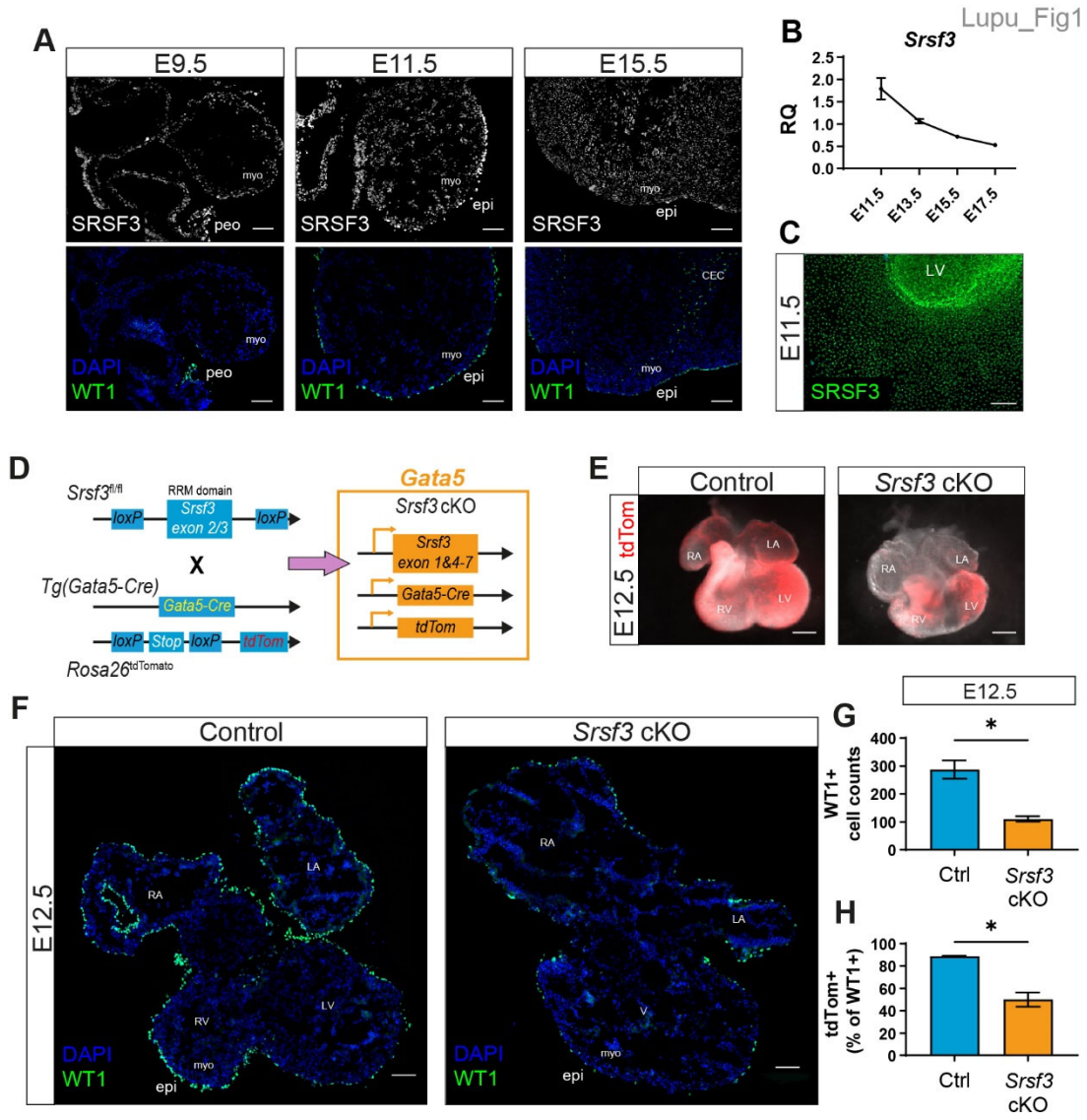

Figure 1. **SRSF3 is expressed in the developing heart and is required for epicardium formation.** (A) Immunofluorescence cryosection images showing expression of SRSF3 and WT1 in embryonic mouse hearts at E9.5, E11.5 and E15.5. Scale bar, 100μm. Images representative of n > 4 embryos. (B) qRT-PCR analysis of *Srsf3* transcript expression in whole heart lysates at E11.5, E13.5, E15.5 and E17.5. Values normalized to Actb. Error bars indicate mean ± SEM (n = 5). (C) Immunofluorescence image showing expression of SRSF3 in a E11.5 epicardial explant. Scale bar, 200μm. Image representative of n = 8 embryos. (D) Generation of a conditional SRSF3 knock-out mouse (*Srsf3* cKO) with lineage tracing capacity; targeting the epicardium lineage (Tg(Gata5-Cre)) and reported by tdTomato ($Rosa26^{tdTomato}$). (E) Fluorescence stereo microscope images of control and *Srsf3* cKO embryonic hearts at E12.5. Epicardial lineage reported by tdTomato fluorescence. Scale bar, 500μm. Images representative of n = 3 embryos. (F) Immunofluorescence cryosection images showing expression of WT1 in control and *Srsf3* cKO embryonic hearts at E12.5. Scale bar, 100μm. Images representative of n = 4 embryos. Quantification of (G) WT1+ cells and (H) percentage tdTomato+ epicardial lineage cells as a proportion of total WT1+ cells. Error bars indicate mean ± SEM (n = 3). Unpaired t-test with Welch's correction (*) P <0.05. *myo; myocardium, peo; proepicardium, epi; epicardium, CEC; coronary endothelial cell, LV; left ventricle. RV; right ventricle, V; ventricles, RA; right atrium, LA; left atrium.*

bioRxiv preprint doi: https://doi.org/10.1101/2021.11.25.470003; this version posted November 25, 2021. The copyright holder for this preprint (which was not certified by peer review) is the author/funder, who has granted bioRxiv a license to display the preprint in perpetuity. It is made available under aCC-BY-NC-ND 4.0 International license.

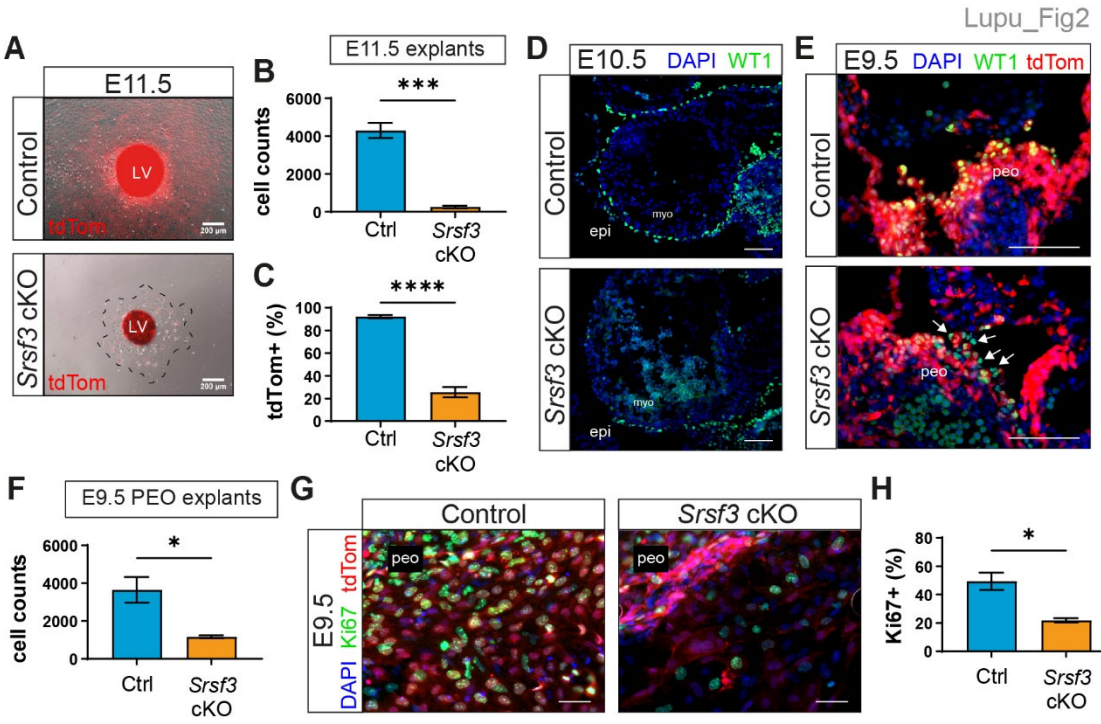

Figure 2**. Impaired proliferation of epicardial progenitor cells in *Srsf3* cKO hearts.** (A) Brightfield and tdTomato fluorescence images of control and *Srsf3* cKO E11.5 ventricular explants (day 3 culture). Scale bar, 200µm. Quantification of (B) epicardial cells and (C) percentage of tdTomato+ cells. Error bars indicate mean ± SEM (n = 6). Unpaired t-test with Welch's correction (***) *P* <0.0001. (D) Immunofluorescence images showing WT1+ cells on the surface of control and *Srsf3* cKO embryonic mouse hearts at E10.5. Scale bar, 100µm. Images representative of n = 3 embryos. (E) Immunofluorescence cryosection images showing WT1+ epicardial progenitor cells situated in the PEO of control and *Srsf3* cKO embryos at E9.5. White arrows highlight non-targeted cells. Scale bar, 100µm. Images representative of n = 5 embryos. (F) Quantification of (pro)epicardial cells from control and *Srsf3* cKO E9.5 PEO explants (day 3 culture). Error bars indicate mean ± SEM (n = 3 - 4). Unpaired t-test with Welch's correction (*) *P* <0.05. (G) Immunofluorescence images and corresponding quantification of (H) percentage Ki67+ (pro)epicardial cells in control and *Srsf3* cKO E9.5 PEO explants (day 3 culture). Scale bar, 50µm. Error bars indicate mean ± SEM (n = 3 - 4). Unpaired t-test with Welch's correction (*) *P* <0.05. *myo; myocardium, peo; proepicardium, epi; epicardium, LV; left ventricle.*

bioRxiv preprint doi: https://doi.org/10.1101/2021.11.25.470003; this version posted November 25, 2021. The copyright holder for this preprint (which was not certified by peer review) is the author/funder, who has granted bioRxiv a license to display the preprint in perpetuity. It is made available under aCC-BY-NC-ND 4.0 International license.

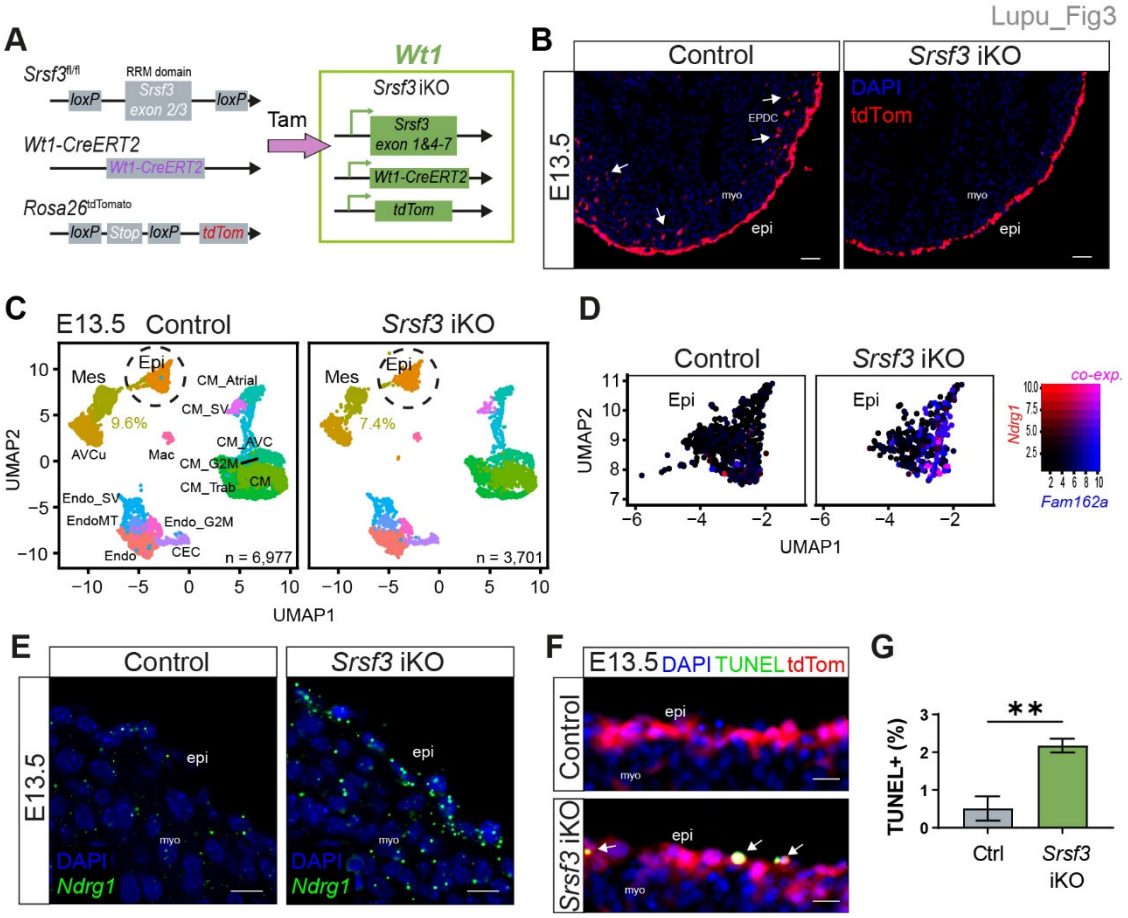

Figure 3. **Impaired proliferation and increased cell death of epicardial cells in *Srsf3* iKO hearts**. (A) Generation of an inducible SRSF3 knock-out mouse (*Srsf3* iKO) with lineage tracing capacity; restricted to the epicardial lineage (*Wt1*-CreERT2) and reported by tdTomato (Rosa26^{tdTomato}). (B) Fluorescence images showing epicardial lineage cells (tdTomato+) in control and *Srsf3* iKO embryonic mouse hearts at E13.5. White arrows highlight invasion of epicardium-derived cells (EPDC) into the myocardium. Scale bar, 50µm. Images representative of n = 6 embryos. (C) UMAP plots showing the major clusters in control and *Srsf3* iKO embryonic mouse hearts at stage E13.5. (D) Feature plots representing range of (co)expression of *Ndrg1* and *Fam162a* mRNA in individual cells of the epicardial (Epi) cluster. Chromium 10X scRNA-seq: control sample; total 6,977 cells, n = 3 hearts, *Srsf3* iKO sample; total 3,701 cells, n = 2 hearts. (E) Fluorescence ISH of *Ndrg1* mRNA in the epicardium of control and *Srsf3* iKO mouse hearts at E13.5. Scale bar, 10µm. Images representative of n = 4 embryos. (F) TUNEL assay cryosection images and corresponding quantification of (G) percentage apoptotic (TUNEL+) epicardial cells in control and *Srsf3* iKO embryonic mouse hearts at E13.5. White arrows highlight apoptotic epicardial cells. Scale bar, 20 µm. Error bars indicate mean ± SEM (n = 4). Unpaired t-test with Welch's correction (**) P <0.01. *myo; myocardium, epi; epicardium, LV; left ventricle, LA; left atrium, Endo; endocardial cells, Epi; epicardium, AVCu; atrioventricular cushion, Mes; mesenchymal cells, CM; cardiomyocytes, CM_Trab; trabecular cardiomyocytes, CM_Atrial; atrial cardiomyocytes, CM_AVC; CM atrioventricular canal, Endo_SV; sinus venosus endocardial cells, EndoMT; endocardial-to-mesenchymal transition cells, CEC; coronary endothelial cells, CM_SV; sinus venosus cardiomyocytes, Mac; macrophages ,_G2M; proliferation cells.*

bioRxiv preprint doi: https://doi.org/10.1101/2021.11.25.470003; this version posted November 25, 2021. The copyright holder for this preprint (which was not certified by peer review) is the author/funder, who has granted bioRxiv a license to display the preprint in perpetuity. It is made available under aCC-BY-NC-ND 4.0 International license.

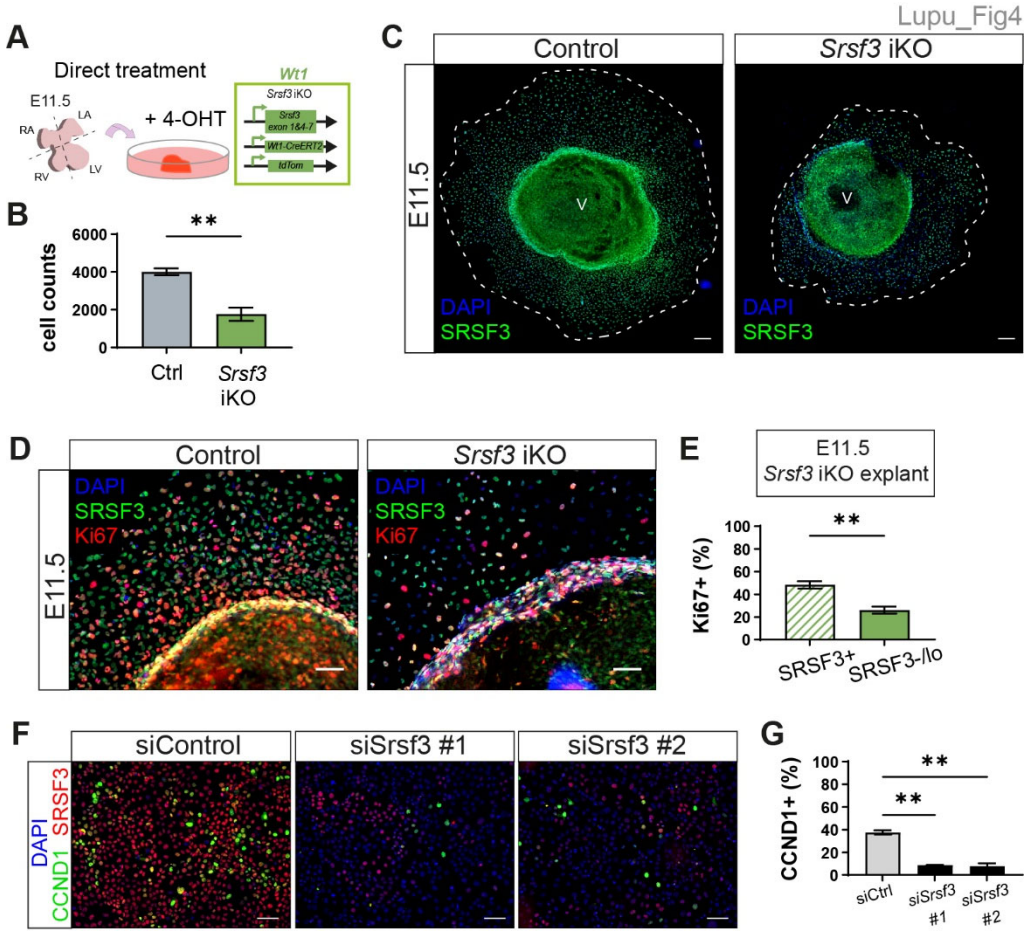

Figure 4. **SRSF3 regulates cell cycle progression in epicardial cell cultures.** (A) Alternate strategy to induce SRSF3 deletion in E11.5 epicardial explants. (B) Quantification of epicardial cells from control and *Srsf3* iKO explants (day 3 culture). Error bars indicate mean ± SEM (n = 4). Unpaired t-test with Welch's correction (**) P <0.01. (C) Immunofluorescence images showing expression of SRSF3 in control and *Srsf3* iKO explants. Scale bar, 200μm. Image representative of n = 4 embryos. (D) Immunofluorescence images and corresponding quantification of (E) percentage Ki67+ epicardial cells as a proportion of SRSF3+ and SRSF3 negative/low (SRSF3-/lo) cells in *Srsf3* iKO explants. Scale bar, 100μm. Error bars indicate mean ± SEM (n = 3). Unpaired t-test with Welch's correction (**) *P* <0.01. (F) Immunofluorescence images and corresponding quantification of (G) percentage CCND1+ epicardial cells in control and *Srsf3* siRNA-trasnsfected cell line. Scale bar, 100μm. Error bars indicate mean ± SEM (N = 3). One-Way Welch ANOVA and Dunnett's multiple comparison test (**) *P* <0.01. *LV; left ventricle. RV; right ventricle, V; ventricle, RA; right atrium, LA; left atrium.*

bioRxiv preprint doi: https://doi.org/10.1101/2021.11.25.470003; this version posted November 25, 2021. The copyright holder for this preprint (which was not certified by peer review) is the author/funder, who has granted bioRxiv a license to display the preprint in perpetuity. It is made available under aCC-BY-NC-ND 4.0 International license.

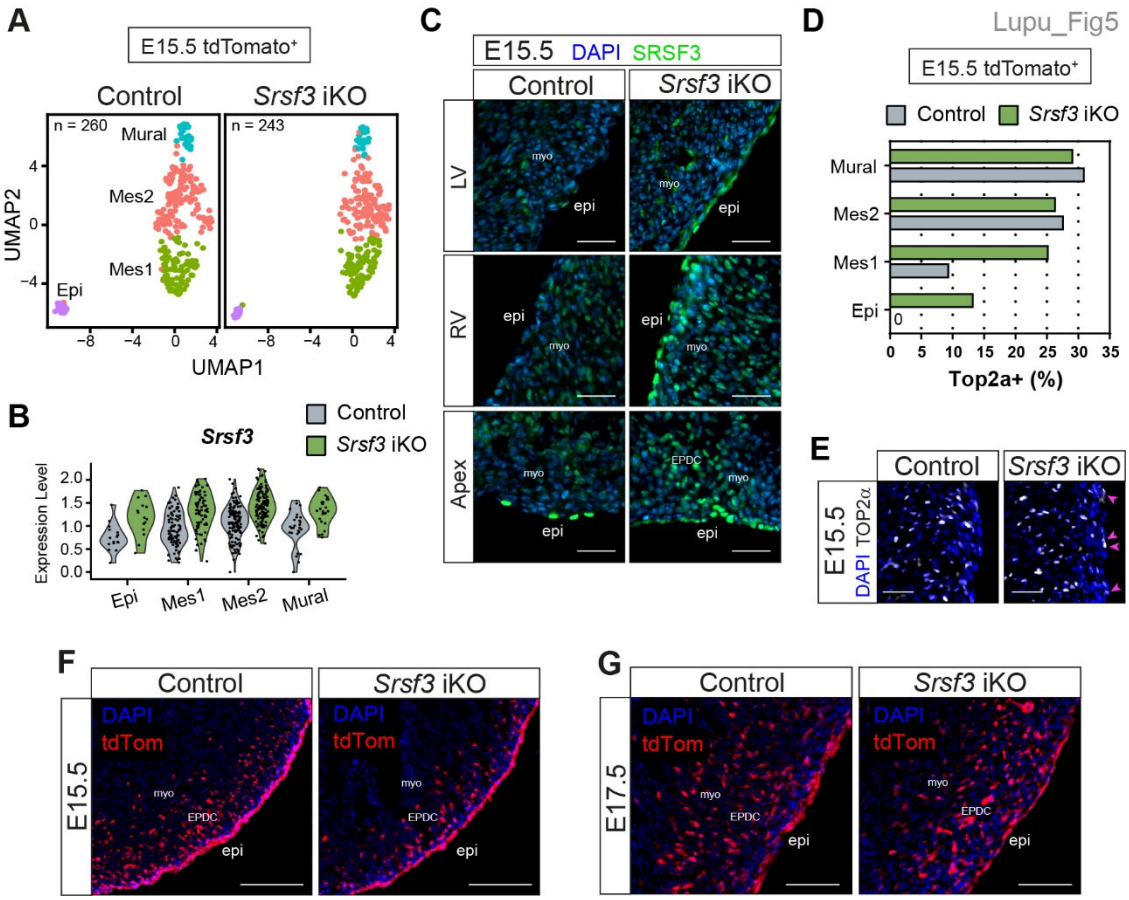

Figure 5. **Non-recombined epicardial lineage cells upregulate SRSF3 and hyperproliferate to compensate for loss of SRSF3-depleted cells in *Srsf3* iKO hearts.** (A) UMAP plots showing the major clusters in epicardial lineage cells of control and *Srsf3* iKO embryonic mouse hearts at E15.5. (B) Violin plot showing relative expression of *Srsf3* in individual clusters. FACS-sorted epicardium lineage (tdTomato+) cells plate-based scRNA-seq: control sample; total 260 cells, n = 6 hearts, *Srsf3* iKO sample; total 243 cells, n = 4 hearts. (C) Immunofluorescence cryosection images showing expression of SRSF3 in the epicardium of control and *Srsf3* iKO embryonic mouse hearts at E15.5. Scale bar, 50μm. Images representative of n = 4 (D) Quantification of percentage *Top2a*-expressing epicardial lineage cells in individual clusters of control and *Srsf3* iKO scRNA-seq data at E15.5. (E) Immunofluorescence cryosection images showing expression of TOP2α in the epicardium of control and *Srsf3* iKO embryonic mouse hearts at E15.5. Magenta arrowheads highlight upregulated expression of TOP2α in epicardial cells. Scale bar, 50μm. Images representative of n = 3. (F, G) Fluorescence images showing epicardial lineage cells (tdTomato+) in control and *Srsf3* iKO embryonic mouse hearts at E15.5 (F) and E17.5 (G). Scale bar, 100μm. Images representative of n = 3 embryos. *myo; myocardium, epi; epicardium, EPDC; epicardium-derived cells, Epi; epicardium cells, Mes; mesenchymal cells.*

bioRxiv preprint doi: https://doi.org/10.1101/2021.11.25.470003; this version posted November 25, 2021. The copyright holder for this preprint (which was not certified by peer review) is the author/funder, who has granted bioRxiv a license to display the preprint in perpetuity. It is made available under aCC-BY-NC-ND 4.0 International license.

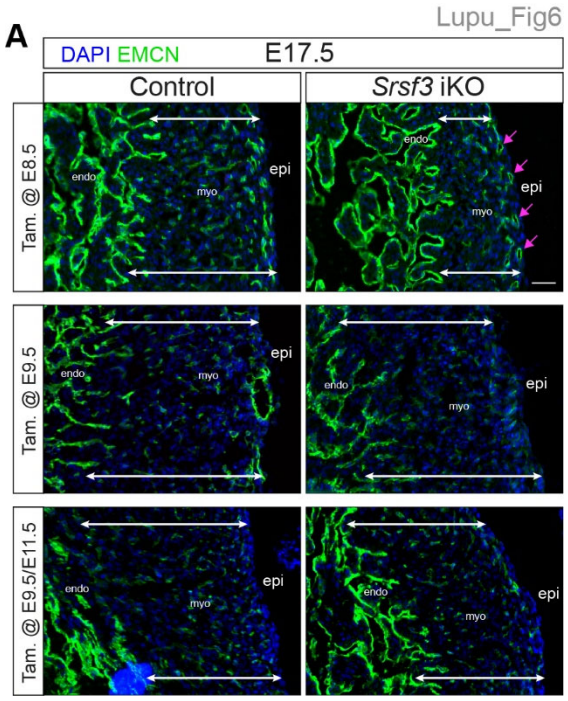

Figure 6. **Defects in compaction and coronary vasculature with early-stage induction of SRSF3 depletion in Srsf3 iKO hearts.** (A) Immunofluorescence cryosection images showing the endocardium and vascular network (EMCN+) in control and *Srsf3* iKO embryonic mouse hearts at E17.5. Tamoxifen induction was administered at E8.5, E9.5, and E9.5/E11.5, respectively. White arrows highlight myocardial wall thickness and magenta arrows highlight presence of superficial vessels. Scale bar, 50μm. Images representative of n = 3 - 4 embryos. *myo; myocardium, epi; epicardium, endo; endocardium.*